# Interval type-2 fuzzy predicates for brain magnetic resonance image segmentation

Diego S. Comas[1, 2], Gustavo J. Meschino[1, 3], Sebastián Costantino[3, 4], Carlos Capiel[3, 4], and Virginia L. Ballarin[1, 3]

[1]*Instituto de Investigaciones Científicas y Tecnológicas en Electrónica, ICYTE, UNMDP-CONICET, Argentina.*
[2]*CONICET (Consejo Nacional de Investigaciones Científicas y Técnicas), Argentina.*
[3]*Universidad Fasta, Argentina.*
[4]*Instituto Radiológico de Mar del Plata, Argentina.*

***Resumen*— El análisis de cambios estructurales en el cerebro por medio de imágenes de resonancia magnética (MRI, del inglés Magnetic Resonance Imaging) aporta información útil para el diagnóstico y el tratamiento clínico de pacientes con patologías tales como enfermedad de Alzheimer y demencia. Aunque la complejidad alcanzada por lo equipos que generan las MRI es cada vez más alto, la cuantificación de estructuras y tejidos no ha sido completamente resuelta. En el presente trabajo, la segmentación de MRI es abordada a través de un nuevo método de clasificación llamado Type-2 Label-based Fuzzy Predicate Classification (T2-LFPC). A partir de datos etiquetados (píxeles de diferentes tejidos de interés seleccionados por expertos médicos) se define una partición aleatoria generando subconjuntos de datos que posteriormente son analizados con el fin de descubrir grupos con propiedades similares, llamados prototipos de clases. Utilizando estos prototipos, se generan funciones de pertenencia tipo 2 de intervalos y predicados difusos y se optimizan los parámetros relacionados a éstos. Luego, los predicados difusos generados son aplicados sobre píxeles sin etiquetar, segmentando las MRI y calculando posteriormente el volumen ocupado por los tejidos de interés dentro de la cavidad intracraneal. Se comparan los resultados obtenidos con los de métodos de clasificación conocidos. Un método para medir la atrofia progresiva y posibles cambios permitiendo comparar efectos terapéuticos debería ser esencialmente automático y, por lo tanto, independiente del radiólogo. Los resultados muestran que el desempeño del método propuesto es altamente aceptable como una contribución para el requerimiento previo. Se discuten las ventajas del enfoque propuesto.***

***Palabras clave*— Volumen encefálico, Predicados difusos, Lógica difusa tipo 2 de intervalos, Imagen de resonancia magnética, segmentación.**

***Abstract*— The analysis of structural changes in the brain through Magnetic Resonance Imaging (MRI) provides useful information for diagnosis and clinical treatment of patients with pathologies like Alzheimer disease and dementia. While complexity achieved by the MRI equipment is high, quantification of structures and tissues has not been entirely solved. In the present paper, MRI segmentation is discussed using a new classification method called Type-2 Label-based Fuzzy Predicate Classification (T2-LFPC). From labeled data (pixels of different tissues selected by medical experts) a random partition is defined and the obtained subsets are analyzed discovering groups with similar properties called class prototypes. Using theses prototypes, interval type-2 membership functions and fuzzy predicates are defined. Parameters regarding the fuzzy predicates are optimized. Fuzzy predicates are applied on unlabeled pixels performing the segmentation and volumes occupied for the tissues into the intracranial cavity are computed. Results are compared to those of known methods. A method of measuring the progressive atrophy and possible changes compared to a therapeutic effect should be essentially automatic and therefore independent of the radiologist. Results show that the performance of the proposed method is highly acceptable as a contribution for this requirement. Advantages of this approach are presented throughout this paper.***

***Keywords*— Brain volume, fuzzy predicates, interval type-2 fuzzy logic, magnetic resonance image, segmentation.**

## I. Introduction

Magnetic Resonance Imaging (MRI) is currently the preferred imaging diagnosis method for the assessment of pathologies of the Central Nervous System (CNS).

The MRI allows obtaining images in multiples views, having high anatomic resolution and the ability of characterizing the brain tissues and their pathologies. These features make MRI clearly superior to other medical imaging types.

The determination of volumes is a useful practice for several diagnoses of nosological entities. Knowing alterations of the standard measurements of the brain volume is very interesting for the differential diagnosis of different pathologies, for assessment of progression and treatment efficacy and monitoring for prognostic evaluation [1].

Volume decreasing can be subjectively assessed, but it is common to find inter-observer discrepancies [2]. Brain MRI allows detecting increase in volumes of the intracranial spaces, normally occupied by Cerebrospinal Fluid (CSF). This increasing is related to the deepening of

Contacto: Diego Sebastián Comas, Laboratorio de Procesamiento Digital de Imágenes at the ICYTE, UNMDP-CONICET, Juan B. Justo 4302, Mar del Plata, Argentina, B7608FDQ, Tel. +54-0223-4816600 int. 255, Fax +54-223-481-0046, *diego.comas@fi.mdp.edu.ar*

sulcus of the brain convexity.

Some neurological diseases may require MRI-based brain volumetric support, such as:

- Alzheimer disease: volumetric alterations can be observed a few years before clinical symptoms coming from typical cognitive alterations appear, like progressive memory loss. Hippocampal atrophy, cingulate and entorhinal cortex atrophy and the later cortical frontoparietal compromise allow recognizing all the stages of the pathology and, therefore, early and advanced neurological affectation relating to them [3].
- Multiple sclerosis: inflammation and demyelinating associated to neurodegenerative processes are the precursors in the probable brain volume loss related to this pathology. Volume loss is bigger than expected in same-age individuals. This volume reduction globally supports some prediction of the disease progress, which makes volume measurement relevant. It begins prematurely and involves not only White Matter (WM), but also cortical Gray Matter (GM) and basal ganglia. A high grade of initial atrophy will lead to diminishing motor and cognitive capacities. No differences are seen between atrophy patterns in different sub-groups of multiple sclerosis [1].
- Frontotemporal dementia: determination of focal atrophy in the anterior sector of frontal and temporal lobes constitutes a marker for the diagnosis of this disease. Subjective observation does not allow assess the low initial volume loss, but it can be properly characterized by volumetric measurements in RM. Two types of frontotemporal dementia develop different atrophy patterns that can be recognized via segmental volumetric assessment, even in early stages, allowing differential diagnosis of entities like Alzheimer disease [4].

By means of image processing techniques, objective volume measurements can be done in MRI, once brain parenchyma could be discriminated from non-parenchyma content. Whether regions of the brain corresponding to the different tissues, i.e. CSF, WM, and GM, are identified, the volume of each tissue can be computed.

There exist some methods to compute brain volumes. Recently an online software was released, named *volBrain* [5], based on multi-atlas label fusion technology. This aims to compute volumes of the intra cranial cavity and those covered by the different tissues. It presents a pipeline including denoising and inhomogeneity correction and the segmentation is based on 50 MRI volumes manually segmented. A discussion of previous approaches for the volume computation can be found in the same work.

Given the previous motivation of brain MRI-based diagnosis, in the present paper brain MRI segmentation is addressed by means of an automatic classification method based on interval type-2 Fuzzy Logic (FL), which is called Type-2 Label-based Fuzzy Predicate Classification (T2-LFPC). From some examples of the different brain tissues (pixels labeled by medical experts), the T2-LFPC method automatically generates a FL predicate system which is used to perform the whole MRI sequence segmentation, detecting pixels of WM, GM, and CSF. Once all pixels are classified, volume of different tissues are computed. Comparisons with other existing classification methods are done, including volume estimation comparison against to the *volBrain* software. In addition, considerations of noise and inhomogeneity field are covered in the FL properties, since it has been proved its robustness to these undesirable effects, considered as data uncertainty [6].

In the next Section, the proposed approach for pixel classification and brain volume estimation is explained and the image acquisition process is described. Then, in Section 3, results are presented and discussed.

## II. Materials and Methods

### *A. Data classification using interval type-2 fuzzy predicates*

FL was introduced by Lofti Zadeh in 1965 [7], [8], extending Boolean (classic) logic in order to deal with vague or imprecise linguistic expressions, considering truth values between 0 (false) and 1 (true). FL provides an effective conceptual framework for dealing with knowledge representation in environments of uncertainty and imprecision like human reasoning and Pattern Recognition [9] and it was successfully applied in image segmentation [6], [10].

The main limitation concerning to traditional FL, called type-1 FL, is that truth values are limited to single values in the [0,1] interval which may not be appropriate for solving problems with great imprecision or when data are affected by noise [9], [11], [12], [13]. In contrast, interval type-2 FL, or interval-valued FL which is the same, provides additional grades of freedom to define truth values using intervals called intervals of truth values [9], [13]. Defining truth values through intervals allows to deal with the effects of noise and to consider opinions of different experts [9], [13]. In previous works, interval type-2 FL was used for Pattern Recognition showing better performance than equivalent models based on type-1 FL [6], [11], [13]–[15].

As it was previously mentioned, in the present work, interval type-2 FL is used for modelling truth values of fuzzy predicates generated by means of the T2-LFPC method, allowing MRI segmentation. In the remainder of the present Section, basics of interval type-2 FL will be introduced in order to provide the necessary notation and concepts for the rest of this paper.

**Definition #1.** An interval of truth values is an interval $A=[a_L, a_R]$, with $0 \le a_L \le a_R \le 1$ [9], [13]. It defines the truth value of a logic expression when interval type-2 FL is used.

**Definition #2.** An interval type-2 membership function $\bar{\mu}_{\mathbf{A}}$ on a discourse universe $U$ is a function $\bar{\mu}_{\mathbf{A}}: U \to \chi$, where $\chi$ is the set of all the closed intervals contained in $[0,1]$, i.e. the set of all the possible intervals of truth values, being $\mathbf{A}$ a property (an attribute) [9], [13]. For a specific value $u \in U$, $\bar{\mu}_{\mathbf{A}}(u)$ is an interval of truth values $\bar{\mu}_{\mathbf{A}}(u)=\left[\varphi^{-}_{\bar{\mu}_{\mathbf{A}}}(u), \varphi^{+}_{\bar{\mu}_{\mathbf{A}}}(u)\right]$ which defines the truth value in which $u$ satisfies the property $\mathbf{A}$. The functions $\varphi^{-}_{\bar{\mu}_{\mathbf{A}}}: U \to [0,1]$ and $\varphi^{+}_{\bar{\mu}_{\mathbf{A}}}: U \to [0,1]$ are strictly type-1 membership functions called respectively the lower and the upper membership functions of $\bar{\mu}_{\mathbf{A}}$ [13].

In FL, a predicate is defined as a property that a variable or a finite collection of variables can have and it is typically assumed as the equivalent of a membership function. In this

work, a fuzzy predicate $p(x)$ is adopted to be the following:

**Definition #3.** A fuzzy predicate $p(x)$, where $x$ indicates an object or a variable, is a declarative sentence which assigns one or more properties to $x$. Considering interval type-2 FL, the value taken by $p(x)$ for a specific value $x = x'$, noted by $\nu(p(x = x'))$, is an interval of truth values $A_{p(x)} = \left[ a_{p(x),L}, a_{p(x),R} \right]$, with $0 \le a_{p(x),L} \le a_{p(x),R} \le 1$.

As in general fuzzy predicates can relate one or more objects or variables with properties, fuzzy predicates can be both simple or compound. Simple predicates directly associate a variable with an attribute and their truth values are usually obtained using membership functions. On the other hand, compound fuzzy predicates logically combine two or more simple predicates using conjunctions ($\wedge$), disjunctions ($\vee$) and complements ($\neg$), which in a wide sense are known as fuzzy aggregation operators. In interval type-2 FL, values of truth of compound predicates are computed using fuzzy conjunctions $C:[0,1]^n \to [0,1]$, disjunctions $D:[0,1]^n \to [0,1]$, and complements $c:[0,1] \to [0,1]$, applied on the ends of the interval of truth values [9], [13]. In the literature, a wide set of different fuzzy conjunctions, disjunctions and complements have been proposed. Selecting different fuzzy operators should be made according to the properties of each operator and how predicates are interpreted and evaluated by the experts in each application. In the case studied in this paper, considering previous results obtained in Pattern Recognition [13], [14], [16]–[18], both MIN-MAX triangular norms and compensatory FL operators are considered [19], [20].

In Pattern Recognition using fuzzy predicates, one or more fuzzy compound predicates combine logically the properties that a datum must meet to belong to a label. By computing the truth value of each predicate explaining the different labels for a datum, the truth value in which the datum belongs to each label is obtained [9], [13]. Label assignment is performed by determining the label for which the datum belongs with highest truth value. In the case of interval type-2 FL, the comparison between truth values requires comparing intervals of truth values and defining which one has the highest truth value.

In [13], a novel methodology for comparing intervals of truth values was proposed, which is based on the concept of measure of interval of truth values. It consists in combining the mean value and the maximum value of an interval in order to obtain a number that globally characterizes the truth value of the interval. In the present paper, this methodology is applied for assigning labels to data representing pixels, performing the MRI segmentation. The concept of measure of interval of truth values is now recalled:

**Definition #4. (Measure of intervals of truth values)**. Let $\chi$ be the set of all the closed intervals contained in $[0,1]$, i.e. the set of all the possible intervals of truth values, the *measure of interval of truth values* [13] is the function $f:\chi \to \mathbb{R}^+$ defined as:

$$f(A) = f\left(\left[a_L, a_R\right]\right) = \frac{a_L + a_R}{2} a_R, \qquad (1)$$

where $A = \left[a_L, a_R\right]$ is an interval of truth values. The function $f$ describes, with a number, the truth value of the interval of truth values, mapping from the interval space to $\mathbb{R}^+$. The higher the value of $f(A)$, the higher the truth value. The reasons of combining the mean value and the maximum of the interval to its characterization are: a) if two intervals have the same mean value, then those with higher maximum value (closer to 1) represents a higher truth value, and b) in the case of two intervals with the same maximum, those with a lower mean value represents a lower truth value.

Considering all the previous definitions, classifiers based on fuzzy predicates are formed by $K$ fuzzy compound predicates, noted by $\left\{p_i(x)\right\}_{i=1,...,K}$, each one associated with one of the possible classes $k \in \{1,...,K\}$. Given a datum $x \in \mathbb{R}^d$ to be assigned to a class, where $d$ is the dimension of the space of patterns, the truth values of the $K$ predicates for $x$ are computed, defining the set $\left\{\nu\left(p_i(x)\right)\right\}_{i=1,...,K}$, where $\nu\left(p_i(x)\right) = \left[a_{p_i(x),L}, a_{p_i(x),R}\right]$ (an interval of truth values). The measure of interval of truth values is applied on each $\nu\left(p_i(x)\right), i = 1,...,K$, resulting in $\left\{f\left(\nu\left(p_i(x)\right)\right)\right\}_{i=1,...,K}$. The label assigned to the datum $x$ is the one whose corresponding fuzzy predicate has the highest measure of interval of truth values, i.e. the class $k$ is assigned to datum $x$ if for the class $k$:

$$\lambda\left(\nu\left(p_k(x)\right)\right) = \max\left\{f\left(\nu\left(p_i(x)\right)\right)\right\}_{i=1,...K}. \qquad (2)$$

Based on the concepts defined in this Section, in the next one the T2-LFPC is explained in detail.

### *B. Method Type-2 Fuzzy Predicate Classification (T2-LFPC)*

As it was previously introduced, brain MRI segmentation is addressed in the present paper using the method T2-LFPC, assigning each pixel of a MRI to one of the classes WM, GM, and CSF. Once pixels are classified with the T2-LFPC, volume estimation is done by each entire MRI sequence. In the present application, each pixel is associated to a data vector composed by a unique variable (its gray level intensity in the T1 sequence) and the different tissues and the background act as labels. Pixel intensity is represented by the gray level of each pixel in each slice.

The next explanation of the method T2-LFPC is presented considering a general classification problem, i.e. not limited to image segmentation. Data to be labeled are represented by $\mathbf{X} \subset [-1,1]^d$, where *N* is the number of data and *d* the number of features, and a datum $\mathbf{x} \in \mathbf{X}$ is a *d*-uple $(x_1, x_2, ..., x_d)$. In addition, $\mathbf{Y} = \{y_r\}_{r=1,...,N}$, $y_r \in \{1,..,K\}$ is the vector of labels (gold-standard) for the data in $\mathbf{X}$, i.e. $\mathbf{X}$ and $\mathbf{Y}$ define the training dataset for the classification problem, being *K* the number of classes (labels).

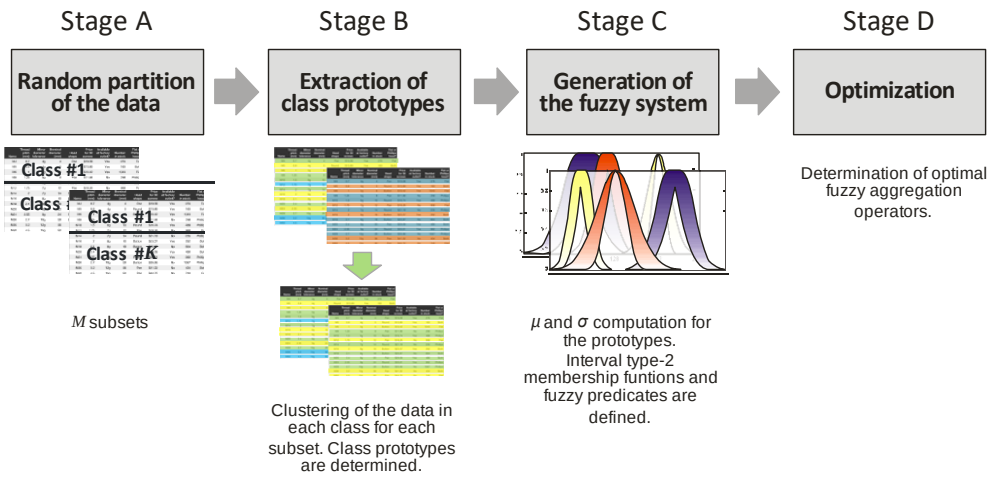


Fig. 1. Processing pipeline of the method T2-LFPC used for brain MRI segmentation.

The Type-2 Label-based Fuzzy Predicate Classification (T2-LFPC) method was originally proposed and used in [14] in order to design nonlinear morphological operators (window morphological operators) for binary images. In the present paper, we propose an improvement of our original method which allows data classification. Considering that the present improvement became the previous method in a general and complete classification method, including the original application of the morphological operator design, we keep the original name, of T2-LFPC. Next, the new T2-LFPC method is explained in detail.

The T2-LFPC method consists of four stages: *A) Random partition of the data*, *B) Extraction of class prototypes*, *C) Generation of the fuzzy system*, and *D) Optimization*. From the training dataset, a classification system based on fuzzy predicates is automatically generated. At Stage A, a random partition of the data is performed. Data contained in each of the obtained subsets are then analyzed at Stage B, applying clustering on data corresponding to each label in order to discover groups of data with similar properties. At Stage C, in each label, the obtained groups are subsequently combined with the other subsets defining interval type-2 membership functions and fuzzy predicates. Finally, at Stage D, parameters of the fuzzy system are optimized. In Fig. 1, the pipeline of the method is shown. Each stage is described in detail in the remainder of this subsection.

*1)* Stage A: Random partition of the data

From the training dataset defined by $\mathbf{X}$ and $\mathbf{Y}$, first, a random partition is performed on $\mathbf{X}$, obtaining $M \geq 2$ disjoint data subsets noted as $\{\mathrm{P}_m\}_{m=1,...,M}$, where $\mathbf{X} = \mathrm{P}_1 \cup \mathrm{P}_2 ... \cup \mathrm{P}_M$. Such random partition is made simultaneously on the label vector $\mathbf{Y}$, given as a result that each $\mathrm{P}_m$ can be written as $\mathrm{P}_m = \Phi_{m,1} \cup \Phi_{m,2} \cup ... \cup \Phi_{m,K}$, where $\Phi_{m,k}$ contains the data in $\mathrm{P}_m$ that belong to the label $k$, $k \in \{1,..,K\}$. The partition is done in such a way that each label has approximately the same quantity of data in the different subsets.

*2)* Stage B: Extraction of class prototypes

In order to define fuzzy predicates and membership functions, it is required an analysis of the properties that presents the data contained in each subset $\Phi_{m,k}$ generated at Stage A. Data corresponding to the same class into a partition do not necessarily share the same properties, i.e. they are not necessarily close in the pattern space.

In order to discover groups with similar properties in $\Phi_{m,k}$, a clustering algorithm is used, discovering groups of data inside of each $\Phi_{m,k}$. Due to the appropriate number of groups for each subset is not known *a priori*, a clustering approach combining Fuzzy C-Means (FCM) clustering [21] and the Bayesian Information Criterion (BIC) is used [22]. This clustering approach allows defining the proper number of clusters for a dataset , being successfully applied in [13], [14]. As a result, each subset $\Phi_{m,k}$ for a label $k$, is divided in $\rho_{m,k}$ clusters.

Formally, the clustering obtained on $\Phi_{m,k}$ can be written as:

$$\Phi_{m,k} = \Delta_{m,k,1} \cup ... \Delta_{m,k,j} ... \cup \Delta_{m,k,\kappa_{m,k}}, \quad (3)$$

where $\Delta_{m,k,j}$ represents data in the cluster $j$ obtained for the data of the label $k$ in the subset $m$, being $k = 1,...,K$ and $m = 1,...,M$. The set of centroids obtained in this stage is noted by $\{\Upsilon_{m,k,j}\}_{\substack{m=1,...,M \\ k=1,...,K \\ j=1,...,\rho_{m,k}}}$.

It is important to note that $\Delta_{m,k,j}$ represents close data in a label $k \in \{1,..,K\}$ in the subset $m$, which were automatically grouped by means of the FCM-BIC clustering approach. Given two subsets $\Delta_{m,k,j_1}$ and $\Delta_{m,k,j_2}$ with $j_1 \neq j_2$, they contain data of $\mathrm{P}_m$ with label $k$ which are not close in the pattern space.

Finally, the data in $\{\Delta_{m,k,j}\}_{\substack{m=1,...,M \\ k=1,...,K \\ j=1,...,\rho_{m,k}}}$ are re-grouped in order to determine the class prototypes. The centroids $\{\Upsilon_{m,k,j}\}_{\substack{m=1,...,M \\ k=1,...,K \\ j=1,...,\rho_{m,k}}}$ are used as data and they are clustered according with their proximity. As a result, the data in $\{\Delta_{m,k,j}\}_{\substack{m=1,...,M \\ k=1,...,K \\ j=1,...,\rho_{m,k}}}$ are clustered again, but this time considering the group assigned to their respective centroids. Explicitly, considering class by class, the subsets

$\left\{\Delta_{m,k,j}\right\}_{\substack{m=1,...,M \\ k=1,...,K \\ j=1,...,\rho_{m,k}}}$ are re-clustered according to their centroids $\Upsilon_{m,k,j}$, with $m$ varying in $1,...,M$ and $j$ varying in $1,...,\rho_{m,k}$ for a class $k$, generating $\kappa_k$ clusters of centroids.

Following the previous procedure, the class prototypes can be determined. The set of class prototypes is noted by $\left\{\Gamma_{k,s,n}\right\}_{\substack{k=1,...,K \\ s=1,...,\kappa_k \\ n=1,...,\zeta_{s,k}}}$, where $k$ is one of the labels $\{1,..,K\}$, $s$ is an index which represents some of the clusters previously obtained for the centroids and $n$ is another index, which corresponds to one of the data subset $\Delta_{m,k,j}, m=1,...,M$, $j=1,...,\rho_{m,k}$, whose centroid was re-assigned to the centroid group $s$ in the previous step, with $s\in\{1,...,\kappa_k\}$.

Using the steps described here, the prototypes in $\Gamma_{k,s,n}$ in a fixed $k$ are data of the training dataset $\mathbf{X}$ which belong to the class $k$. All the data of the class $k$ are in one of the sets $\left\{\Gamma_{k,s,n}\right\}_{\substack{s=1,...,\kappa_k \\ n=1,...,\zeta_{s,k}}}$. Likewise, $\Gamma_{k,s,n}$ for specific $k$ and $s$, contains $\zeta_{s,k}$ clusters of data, each near to each other, where each group of data contains examples of the class $k$ which share same properties, i.e. they are close in the pattern space.

*3)* Stage C: Generation of the fuzzy system

From stages *A* and *B*, the data of each class were clustered in subsets having similar properties and resulting in class prototypes. In the present stage, the prototypes in $\left\{\Gamma_{k,s,n}\right\}_{\substack{k=1,...,K \\ s=1,...,\kappa_k \\ n=1,...,\zeta_{s,k}}}$ are analyzed, defining interval type-2 membership functions and fuzzy predicates generating a FL system which allows to classify data.

First, for each set of class prototype $\Gamma_{k,s,n}$, with $n=1,...,\zeta_{s,k}$ and fixed $k$ and $s$, a Gaussian type-1 membership function is found. Centroids of the membership functions noted by $\Omega_{k,s,n}$ are obtained as the centroid of the data in each $\Gamma_{k,s,n}$. As a result, for a label $k$ in a prototype group $s$, $\zeta_{s,k}$ type-1 membership functions are defined for each feature $i\in\{1,...,d\}$. Widths of the membership functions are computed as the standard deviation of the data in $\Gamma_{k,s,n}$ for each class $k$ in each group $s=1,...,\kappa_k$. The standard deviation is a parameter, controlling how the truth value of the membership functions decreases when the values move away from the centroid found for the class prototypes. The type-1 membership functions are noted by $\left\{\mu_{i,k,s,n}\right\}_{\substack{i=1,...,d \\ k=1,...,K \\ s=1,...,\kappa_k \\ n=1,...,\zeta_{s,k}}}$.

As it was previously mentioned, the class prototypes $\Gamma_{k,s,n}$ share the same properties for fixed values of $k$ and $s$. After type-1 membership functions are defined, these are aggregated varying the parameter $n$, as follow:

$$\varphi^{-}_{\hat{\bar{\mu}}_{i,k,s}}(x)=\min\left\{\mu_{i,k,s,n}(x)\right\}_{n=1,...,\zeta_{s,k}},\ \forall x\in[-1,1], \quad (4)$$

$$\varphi^{+}_{\hat{\bar{\mu}}_{i,k,s}}(x)=\max\left\{\mu_{i,k,s,n}(x)\right\}_{n=1,...,\zeta_{s,k}},\ \forall x\in[-1,1], \quad (5)$$

$\forall x\in[-1,1]$, $i\in\{1,...,n\}$, $k\in\{1,...,K\}$, $s=1,...,\kappa_k$, where $\varphi^{-}_{\hat{\bar{\mu}}_{i,k,s}}:[-1,1]\to[0,1]$ and $\varphi^{+}_{\hat{\bar{\mu}}_{i,k,s}}:[-1,1]\to[0,1]$ are respectively the lower and the upper membership functions of an interval type-2 membership function $\hat{\bar{\mu}}_{i,k,s}:[-1,1]\to\chi$, defining with what truth value the feature $i$ of a datum belong to the class $k$ according to the set of prototypes $s$. As it is easy to note, $\hat{\bar{\mu}}_{i,k,s}(x)$ is the interval of truth value $\left[\varphi^{-}_{\hat{\bar{\mu}}_{i,k,s}}(x),\varphi^{+}_{\hat{\bar{\mu}}_{i,k,s}}(x)\right]$.

The obtained interval type-2 membership functions $\hat{\bar{\mu}}_{i,k,s}, i=1,...,d, k=1,...,K, s=1,...,\kappa_k$ are then smoothed, using a numerical interpolation, trying to eliminate possible peaks generated by the MIN-MAX aggregation. This procedure defines new interval type-2 membership functions $\left\{\bar{\mu}_{i,k,s}\right\}_{\substack{i=1,...,d \\ k=1,...,K \\ s=1,...,\kappa_k}}$ [23].

Finally, fuzzy predicates for each class $k\in\{1,...,K\}$ are defined by logically operating, according to the index $i$ which represents the feature, with the truth values described by the membership functions $\left\{\bar{\mu}_{i,k,s}\right\}_{\substack{i=1,...,d \\ k=1,...,K \\ s=1,...,\kappa_k}}$. Considering the class $k$, $\kappa_k$ compound fuzzy predicates are defined, each one associated with properties of the data belonging to the class $k$ in the training dataset $\mathbf{X}$. These predicates are:

$$p_{k,s}(\mathbf{x})\equiv\bar{\mu}_{1,k,s}(x_1)\wedge\bar{\mu}_{2,k,s}(x_2)\wedge,\ldots,\wedge\,\bar{\mu}_{d,k,s}(x_d),\quad k=1,2,\ldots,K,\ s=1,...,\kappa_k, \quad (6)$$

where $\mathbf{x}$ is a datum and the value of $p_{k,s}(\mathbf{x})$ defines the truth value in which $\mathbf{x}$ belong to the class $k$. The predicates $\left\{p_{k,s}\right\}_{s=1,...,\kappa_k}$ are combined in a fuzzy predicate $p_k(\mathbf{x})$ using the disjunction operator ($\vee$), obtaining a unique fuzzy predicate for each class as following:

$$p_k(\mathbf{x})\equiv p_{k,1}(\mathbf{x})\vee\,p_{k,2}(\mathbf{x})\vee,\ldots,\vee\,p_{k,\kappa_k}(\mathbf{x}),\quad k=1,2,\ldots,K. \quad (7)$$

As a result, interval type-2 membership functions and fuzzy predicates are generated, respectively noted by $\left\{\bar{\mu}_{i,k,s}\right\}_{\substack{i=1,...,d \\ k=1,...,K \\ s=1,...,\kappa_k}}$ and $\left\{p_k\right\}_{k=1,...,K}$, which are obtained from the training dataset $\{\mathbf{X},\mathbf{Y}\}$, defining a FL system. This system can be used both to classify the data in $\mathbf{X}$ as well as other data resulting of the same process that generated the set $\mathbf{X}$ (generalization).

Fuzzy predicates are evaluated using fuzzy aggregation operators and classes are assigned following the procedure detailed at the end of the Section II.*A*.

*4)* Stage D: Optimization

Using the training dataset $\{\mathbf{X},\mathbf{Y}\}$, it is possible to compute the training error (or resubstitution error) [24] once the FL system was generated. Thus, by quantifying the training error it is possible to properly set parameters of the fuzzy system such as the aggregation operators used to evaluate the conjunction and disjunction in the predicates.

As final step, the FL system is used to classify the training data, testing the aggregation operators MIN-MAX and the compensatory ones, both based in the geometric mean [19] and the arithmetic mean [20]. The classification error is computed in each case as a percentage of incorrected classified data and considering as gold-standard the labels in $\mathbf{Y}$.

As a result, a FL system is obtained, enabling to classify data of the same kind that the training dataset $\{\mathbf{X}, \mathbf{Y}\}$. The FL system is formed by interval type-2 membership functions and fuzzy predicates, explaining the classes to be obtained and defining the optimal parameters for the predicate evaluation. Only the size of initial partition $M$ must be defined, which must be determined heuristically in accordance with the quantity of available data [13], [14].

### C. Volume estimation

Volume estimation requires the following steps: intracranial cavity segmentation, tissue classification and volume computation. The performance of each stage influences dramatically the following ones.

There are plenty of methods for the intracranial cavity segmentation. Many of them have been compared in previous works [25]. In this paper, a method based on the application of Mathematical Morphology is used, which consists of using sequential filters by reconstruction with structuring elements of growing size [26]. Apart from enhancing and filtering the image, this method captures the interior of a closed simple curve employing geodesic distance. This curve represents the external brain boundary.

Once intracranial cavity area is determined for each slice, an expert selects small regions in random slices to construct a training dataset, i.e. a gold-standard. The expert selects regions for the different classes: GM, WM, and CSF. Background, i.e., pixels that does not belong to any of the considered tissues, is not selected in this stage due to this was previously removed during the segmentation of the intracranial cavity.

As a result, a training dataset is defined $\{\mathbf{X}, \mathbf{Y}\}$, formed by the intensities of the pixels defined by the MRI in the T1 sequence and the corresponding labels defined by the expert. Then, the method T2-LFPC is applied assigning pixels to one and only one of the classes GM, WM, and CSF.

Once FL system is generated from the examples defined in the training dataset $\{\mathbf{X}, \mathbf{Y}\}$, the system is used to classify all the pixels in the entire volume.

In order to compute the volume of each issue, first, the volume of a single voxel is determined, considering the distance inter-slices (slice thickness) and the pixel spacing (in both directions), assuming that each pixel represents a voxel. The product between these three values is the unitary voxel volume represented by one pixel. Finally, the volume occupied by each tissue is obtained as the number of voxels belonging to the tissue times the unitary voxel volume.

### D. Image databases

The method T2-LFPC was initially tested with images coming from Montréal Neurological Institute Simulated Brain Database, McGill University [27]. Only simulated T1-weighed images were considered in order to make possible an extrapolation of the results to real images. Since these simulations have a gold-standard, the performance of the classification method could be assessed by a quality measure. Dimensions for the volume were 181x217x181 voxels, noise levels: 0%, and levels of intensity non-uniformity (INU): 0%.

The second image database came from a diagnostic imaging center, considering real cases, patients with known pathologies and MRI in T1 sequence. Images were acquired in a Philips equipment, 1.5 Tesla. Dimensions for the volume were 320x320x160 voxels, resolution 12 bits, in sagittal view. Pixel spacing was 0.8 x 0.8 millimeters and slice thickness was 1 millimeter, defining a unitary voxel volume of 0.64 cubic millimeters ($0.64 \times 10^{-3}$ cubic centimeters). Volumes were processed considering slices in axial view.

In this case, gold-standards are not available for the entire volume, but a gold-standard was made by experts considering some pixels taken of some slices and labeling them as GM, WM, or CSF, defining the training dataset. Volume results were compared against the results of the online software *volBrain* [5]. Classification performance is detailed in the next Section.

### E. Quality measurements

In order to assess the segmentation results, accuracy was chosen as quality measurement, defined as the percentage of pixels correctly classified. Accuracy was computed considering the generalization abilities of the classifiers: once trained the classifiers, accuracy was computed with the output of the classifiers for new data not contained in the training dataset.

In the simulated MRI volume, first, 100 pixels per tissue were randomly selected of the entire volume, defining the training dataset. Then, the classifier was applied to segment the first slice of the volume (considered as test dataset), computing the accuracy for that slice. This procedure was repeated for each slice in the volume, defining in each case a new training dataset. The average of the obtained accuracies is reported, including the standard deviation.

As it was pointed-out before, for the real MRI volumes gold-standards were not available for the whole slices, but quality measures were computed for the pixels in the training set. From the total of pixels labeled by the medical experts, 200 pixels per tissue were randomly selected, defining the training dataset with 600 data. A 10-fold cross validation was considered in order to estimate the generalization abilities of the classifiers [28]. Then, the entire volume was processed using all the training dataset.

## III. Results

In this Section, results for slice segmentation and volume computation are presented, considering both the simulated and the real MRI volumes.

In Fig. 2, results obtained using T2-LFPC for three slices (corresponding to #22, #35 and #100) for the simulated images are shown. In this case, as gold-standards were available, these are included in the third column for visual purposes. A comparison against to known classification methods was performed, considering the K-nearest Neighbor Algorithm (KNN), MultiLayer Perceptron (MLP), Probabilistic Neural Networks (PNN) and a similar method to the T2-LFPC, but using type-1 FL, called Type-

1 Label-based Fuzzy Predicate Classification (T1-LFPC). Unlike the T2-LFPC, type-1 membership functions are not aggregated. Instead, these are directly used generating a type-1 FL system. These methods were heuristically parametrized, testing different setting. Reported results are the best results obtained for each classifier, considering the average accuracy for the different setting parameters.

Accuracy results for the segmentation are shown in Table I. Standard deviations were computed along the slices. MLP gave the best in terms of mean accuracy and standard deviation. However, the method T2-LFPC presents a good trade between accuracy and computation times and differences were not statistically significant after computing *P* using the non-parametrical Wilcoxon test. Besides, previous deeper studies allowed concluding that T2-LFPC showed the best performance considering noise and distortion in images. In addition, methods based on fuzzy predicates allow to give a deeper understanding about the classification obtained, which could be helpful for image interpretation [13]. However, these discussions are far beyond the scope of this paper.

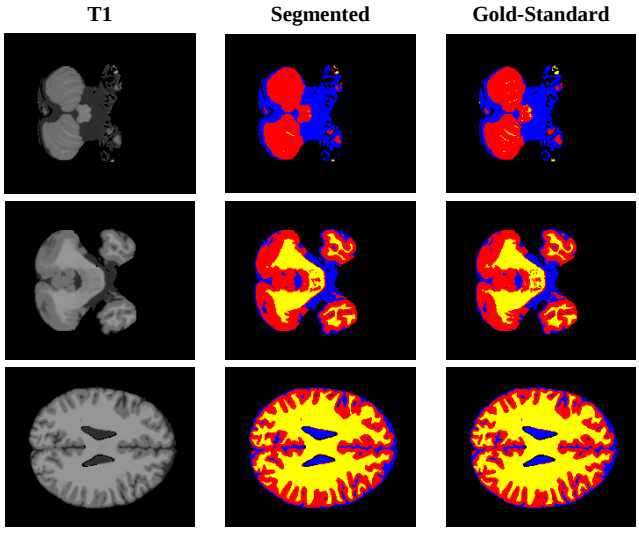


Fig. 2. Segmentation obtained for three slices in simulated MRI volumes. The first column shows T1 images after intracranial cavity extraction, second column shows the results obtained by using the T2-LFPC method and the last column shows the gold-standards.

In Fig. 3, three slices of the real MRI images, corresponding to the slices #44, #100 and #200, are presented. In the third column of this figure, segmentation was superimposed to the original images. The method T2-LFPC is compared to KNN, MLP, PNN, and T1-LFPC, considering different setting parameters in each case. Results presented correspond to the best performance for each method, determined according to the accuracies estimated using 10-fold cross validation applied on the pixels in the training set. The estimated accuracies and its standard deviation are shown in Table II. Differences among the different methods were statistically not significant, showing KNN the best performance.

For the MRI volume presented in Table II and Fig. 3, volume of the intracranial cavity and volumes and percentages covered by the different tissues were computed for the T2-LFPC method and the test methods, comparing the results against to the results of the online software *Volbrain* [5]. These results are presented in Table III.

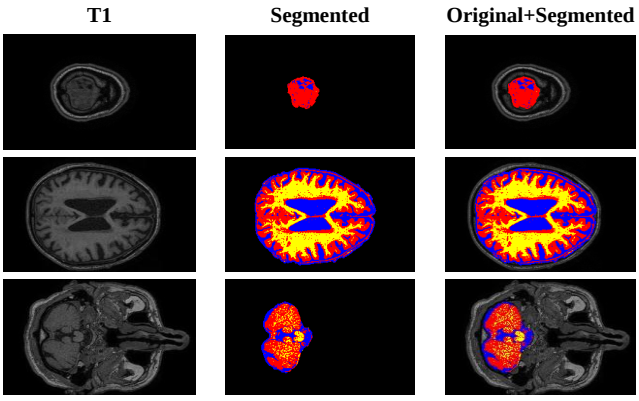


Fig. 3. Segmentation obtained for three slices of the real MRI volume. The first column shows T1 images before intracranial cavity extraction, second column shows the results obtained from the method T2-LFPC and third column shows results superimposed to original images.

TABLE I
ACCURACY FOR THE SIMULATED MRI VOLUME.

| | **T2-LFPC** | KNN | MLP | PNN | T1-LFPC |
|---|---|---|---|---|---|
| Mean | **0.975** | 0.976 | 0.981 | 0.977 | 0.972 |
| Standard deviation | **0.009** | 0.009 | 0.007 | 0.008 | 0.010 |
| Computation time [s] | **65** | 28 | 550 | 141 | 57 |

T2-LFPC: Proposed method. KNN: K-Nearest Neighbor. MLP: MultiLayer Perceptron. PNN: Probabilistic Neural Network. T1-LFPC: Method similar to T2-LFPC using type-1 FL. Computation time includes training and segmentation of the entire volume.

TABLE II
ACCURACY FOR THE REAL MRI VOLUME.

| | **T2-LFPC** | KNN | MLP | PNN | T1-LFPC |
|---|---|---|---|---|---|
| Mean | **0.943** | 0.950 | 0.948 | 0.942 | 0.938 |
| Standard deviation | **0.027** | 0.021 | 0.029 | 0.029 | 0.026 |
| Computation time [s] | **0.449** | 0.133 | 13.064 | 1.057 | 0.349 |

T2-LFPC: Proposed method. KNN: K-Nearest Neighbor. MLP: MultiLayer Perceptron. PNN: Probabilistic Neural Network. T1-LFPC: Method similar to T2-LFPC using type-1 FL. Computation time includes training and segmentation of one slice.

The determination of the intracranial cavity is crucial to estimate the percentages of each tissue. In the methods considered in this paper, this volume is constant because the same method for intracranial cavity segmentation was applied in all cases.

An objective comparison of these results is a difficult task, because there is no gold-standard. But the observed consistency between results and the subjective expert assessment of the segmented slices are good evidence about the reliability of the results.

## IV. CONCLUSION

In this paper, the method Type-2 Label-based Fuzzy Predicate Classification (T2-LFPC) is presented and is applied to segmentation of brain magnetic resonance images. Results for slice segmentation and volume computation were presented, considering both simulated and real MRI volumes. A comparison against other known methods was performed, considering the k-nearest neighbor algorithm, multilayer perceptron, probabilistic neural networks, and a similar method to the T2-LFPC but using type-1 FL (T1-LFPC). The method T2-LFPC showed a good trade between accuracy and computation times, and

TABLE III

COMPARISON OF RESULTS OBTAINED BY THE PROPOSED METHOD AGAINST TO THOSE OBTAINED WITH OTHER CLASSIFICATION METHODS AND THE ONLINE SOFTWARE *VOLBRAIN* [5]. VOLUMES ARE EXPRESSED BOTH IN $CM^3$ AND IN PERCENTAGE

| | **T2-LFPC** | KNN | MLP | PNN | T1-LFPC | Volbrain |
|---|---|---|---|---|---|---|
| White Matter (WM) | **400.22 (22.93%)** | 376.39 (21.57%) | 397.29 (22.77%) | 413.75 (23.71%) | 371.22 (21.27%) | 408.42 (23.63%) |
| Grey Matter (GM) | **760.48 (43.58%)** | 786.50 (45.07%) | 734.95 (42.11%) | 727.52 (41.69%) | 816.00 (46.76%) | 759.28 (43.92%) |
| Cerebro Spinal Fluid (CSF) | **584.44 (33.49%)** | 582.25 (33.36%) | 612.91 (35.12%) | 603.87 (34.60%) | 557.92 (31.97%) | 561.06 (32.45%) |
| Brain (WM + GM) | **1160.70 (66.51%)** | 1162.89 (66.64%) | 1132.24 (64.88%) | 1141.27 (65.40%) | 1187.23 (68.03%) | 1167.70 (67.55%) |
| Intracranial Cavity (IC) | **1745.14 (100.00%)** | 1745.14 (100.00%) | 1745.14 (100.00%) | 1745.14 (100.00%) | 1745.14 (100.00%) | 1728.74 (100.00%) |

differences with the test methods were not statistically significant considering the non-parametrical Wilcoxon test.

The comparison allowed concluding that the method T2-LFPC showed good performance considering noise and distortion in images. In addition, methods based on fuzzy predicates give a deeper understanding about the classification obtained, which could be helpful for image interpretation.

A method of measuring the progressive atrophy and possible changes compared to a therapeutic effect should be essentially automatic and therefore independent of the radiologist. The approach of the method followed in this paper is a valuable contribution to achieve this ambitious goal. Future work will include a major analysis of the stage involve in the method T2-LFPC as well as tests on new real MRI volumes and comparisons against methods specifically adjusted for brain MRI segmentation.

## ACKNOWLEDGEMENT

Diego S. Comas acknowledges support from Consejo Nacional de Investigaciones Científicas y Técnicas (CONICET) from Argentina.

## REFERENCES

[1] M. P. Wattjes, M. D. Steenwijk, and M. Stangel, "MRI in the Diagnosis and Monitoring of Multiple Sclerosis: An Update.," *Clin. Neuroradiol.*, vol. 25 Suppl 2, pp. 157–65, Oct. 2015.

[2] C. W. Kanaly *et al.*, "A novel, reproducible, and objective method for volumetric magnetic resonance imaging assessment of enhancing glioblastoma.," *J Neuosurg*, vol. 76, no. 6, pp. 1–7, 2014.

[3] K. A. Johnson, N. C. Fox, R. A. Sperling, and W. E. Klunk, "Brain imaging in Alzheimer disease.," *Cold Spring Harb. Perspect. Med.*, vol. 2, no. 4, p. a006213, Apr. 2012.

[4] J. D. Rohrer, "Structural brain imaging in frontotemporal dementia," *Biochim. Biophys. Acta - Mol. Basis Dis.*, vol. 1822, no. 3, pp. 325–332, 2012.

[5] J. V. Manjón and P. Coupé, "volBrain: An Online MRI Brain Volumetry System," *Front. Neuroinform.*, vol. 10, p. 30, Jul. 2016.

[6] D. S. Comas, G. J. Meschino, J. I. Pastore, and V. L. Ballarin, "A survey of medical images and signal processing problems solved successfully by the application of Type-2 Fuzzy Logic," *J. Phys. Conf. Ser.*, vol. 332, p. 12030, 2011.

[7] L. A. Zadeh, "Fuzzy sets," *Inf. Control*, vol. 8, pp. 338–353, 1965.

[8] L. A. Zadeh, "The Concept of a Linguistic Variable and its Application to Approximate Reasoning," *Inf. Sci. (Ny).*, vol. 8, pp. 199–249, 1975.

[9] D. S. Comas, J. I. Pastore, A. Bouchet, V. L. Ballarin, and G. J. Meschino, "Type-2 Fuzzy Logic in Decision Support Systems," in *Soft Computing for Business Intelligence*, vol. 537, no. 537, R. A. Espin Andrade, R. Bello Pérez, Á. Cobo, J. Marx Gómez, and A. Racet Valdés, Eds. Heidelberg, Germany: Springer Berlin Heidelberg, 2014, pp. 267–280.

[10] G. J. Meschino, R. A. Espin Andrade, and V. L. Ballarin, "A framework for tissue discrimination in Magnetic Resonance brain images based on predicates analysis and Compensatory Fuzzy Logic," *Int. J. Intell. Comput. Med. Sci. Image Process.*, vol. 2, no. X, pp. 1–16, 2008.

[11] P. Melin and O. Castillo, "A review on the applications of type-2 fuzzy logic in classification and pattern recognition ," *Expert Syst. Appl.*, vol. 40, no. 13, pp. 5413–5423, 2013.

[12] J. M. Mendel, "Type-2 fuzzy sets and systems: an overview," *IEEE Comput. Intell. Mag.*, vol. 2, no. 1, pp. 20–29, 2007.

[13] D. S. Comas, G. J. Meschino, A. Nowé, and V. L. Ballarin, "Discovering knowledge from data clustering using automatically-defined interval type-2 fuzzy predicates," *Expert Syst. Appl.*, vol. 68, pp. 136–150, 2017.

[14] D. S. Comas, G. J. Meschino, M. Brun, and V. L. Ballarin, "Label-based Type-2 Fuzzy Predicate Classification applied to the design of morphological W-operators for image processing," in *First Latin American Congress on Computational Intelligence*, 2014, pp. 55–60.

[15] D. S. Comas, G. J. Meschino, A. Nowe, and V. L. Ballarin, "Knowledge discovering in data clustering by self-discovered type-2 fuzzy predicates," in *Fifth international workshop on Knowledge Discovery, Knowledge Management and Decision Support (Eureka 2015)*, 2015.

[16] G. J. Meschino, D. S. Comas, V. L. Ballarin, A. G. Scandurra, and L. I. Passoni, "Using SOM as a Tool for Automated Design of Clustering Systems Based on Fuzzy Predicates," in *9th Workshop on Self-Organizing Maps (WSOM 2012)*, 2012, pp. 85–94.

[17] G. J. Meschino, D. S. Comas, V. L. Ballarin, A. G. Scandurra, and L. I. Passoni, "Automatic design of interpretable fuzzy predicate systems for clustering using self-organizing maps," *Neurocomputing*, vol. 147, no. 1, 2015.

[18] D. S. Comas, G. J. Meschino, and V. L. Ballarin, "Discovering type-2 fuzzy predicates in data guided by automatic clustering algorithms," in *Eureka International Virtual Physical Meeting 2014*, 2014.

[19] R. A. Espin Andrade, G. MazcorroTéllez, E. Fernández González, J. Marx-Gómez, and M. I. Lecich, "Compensatory Logic: a fuzzy normative model for decision making," vol. 27, no. 2, pp. 178–193, 2006.

[20] A. Bouchet, J. I. Pastore, R. E. Andrade, M. Brun, and V. Ballarin, "Arithmetic Mean Based Compensatory Fuzzy Logic," *Int. J. Comput. Intell. Appl.*, vol. 10, no. 2, pp. 231–243, 2011.

[21] J. C. Bezdek, R. Ehrlich, and W. Full, "FCM: The fuzzy c-means clustering algorithm," *Comput. Geosci.*, vol. 10, no. 2–3, pp. 191–203, 1984.

[22] C. Fraley and A. E. Raftery, "How Many Clusters? Which Clustering Method? Answers Via Model-Based Cluster Analysis," *Comput. J.*, vol. 41, no. 8, pp. 578–588, 1998.

[23] D. S. Comas, J. I. Pastore, A. Bouchet, V. L. Ballarin, and G. J. Meschino, "Interpretable interval type-2 fuzzy predicates for data clustering: A new automatic generation method based on self-organizing maps," *Knowledge-Based Syst.*, vol. 133, pp. 234–254, Oct. 2017.

[24] C. Sima, S. Attoor, U. Brag-Neto, J. Lowey, E. Suh, and E. R. Dougherty, "Impact of error estimation on feature selection," *Pattern Recognit.*, vol. 38, no. 12, pp. 2472–2482, 2005.

[25] G. Ridgway, J. Barnes, T. Pepple, and N. Fox, "Estimation of total intracranial volume; a comparison of methods," *Alzheimer's Dement.*, vol. 7, no. 4, pp. S62–S63, 2011.

[26] J. I. Pastore, E. G. Moler, and V. L. Ballarin, “Segmentation of brain magnetic resonance images through morphological operators and geodesic distance,” *Digit. Signal Process.*, vol. 15, no. 2, pp. 153–160, 2005.
[27] B. Aubert-Broche, A. C. Evans, and L. Collins, “A new improved version of the realistic digital brain phantom.,” *Neuroimage*, vol. 32, no. 1, pp. 138–45, Aug. 2006.
[28] E. R. Doughtery, H. Jianping, and M. L. Bittner, “Validation of computational methods in genomics.,” *Curr. Genomics*, vol. 8, no. 1, pp. 1–19, Mar. 2007.